DOI 10.1007/s11223-021-00263-5
Strength of Materials, Vol. 53, No. 1, January, 2021

CORROSION MECHANISM OF A PLASMA NITRIDING–TREATED ALLOY

Z. L. Peng[1] and H. M. Zhao UDC 539.4

Plasma nitriding of an alloy is a low-temperature chemical-thermal treatment technology. The nitrided layer exhibits a high density, corrosive, wear, and fatigue resistance, being low-deformable. A 12Cr2NiWVA alloy was plasma-nitrided, and the corrosion mechanism of the nitrided layer at high temperature and pressure was studied. The effect of nitriding, heat treatment, fine grinding, and other technologies on corrosion was investigated. The composition of a corroded material was analyzed, and sectional hardness was microscopically examined. It is demonstrated that nitriding not only improved the wear resistance but also reduced the chromium content in the matrix, resulting in the reduction of the oxidation and corrosive resistance performances of the material. Fine grinding exerted an adverse effect on the wear and corrosive resistance. The varying distribution of temperatures during the heat treatment resulted in the nonuniformity of properties throughout the material after nitriding, followed by the growth of strains.

Keywords: corrosion mechanism, 12Cr2NiWVA alloy, plasma nitriding.

Introduction. Nitriding is a surface chemical processing technology by which nitrogen will permeate the surface of a specimen surrounded by a nitrogen-containing medium at a certain temperature. As a consequence, a layer of nitride will be generated to change the performance of the processed specimen. Generally, the treated specimen has advantageous characteristics such as corrosion resistance, high hardness, and small-scale deformation [1, 2].

Plasma nitriding applies glow discharge of a thin nitrogen-containing gas between a specimen (cathode) and an anode in 10^{-3}–10^{-2} Torr N_2–H_2 or NH_3 or pure N_2 ambience based on the glow discharge of gases [3–5]. Effects of the alloying layer, phase, and alloying elements on the alloying layer of the plasma-nitrided alloy are the same as those of the regular gas-nitrided alloy. However, defect structures and morphologies of the phases in the plasma nitriding layer are different, and hence the performances after treatment are also different.

Thermal erosion of alloy is serious surface corrosion of the matrix metal under high-temperature gas action [6, 7]. Typically, thermal erosion occurs under conditions of the complex chemical, thermodynamic and hydrodynamic effects of dust, water vapor, various ions, and other impurities in flue gas, which is also called exhaust gas) [8, 9], causing pits and residues due to the corrosion and hence resulting in the failure of a component [10]. Therefore, it is interesting to study the corrosion mechanism for delaying corrosion, maintaining technical performance, and improving the reliability of components.

1. Materials and Procedures. A cylinder liner made of the 12Cr2NiWVA alloy was treated by hardening–tempering, plasma nitriding, and fine grinding successively. The cylinder liner worked at the highest flue gas temperature of 1200℃ and flue gas pressure of 28 MPa and cooled by water. In order to ensure the dimensional accuracy and surface finish, the internal surface of the cylinder liner was subjected to grinding. After working for 24 h, the cylinder liner was seriously corroded.

College of Mechatronic Engineering, North University of China, Shanxi Taiyuan, China ([1]pengzhiling@nuc.edu.cn). Translated from Problemy Prochnosti, No. 1, pp. 85 – 88, January – February, 2021. Original article submitted February 3, 2020.

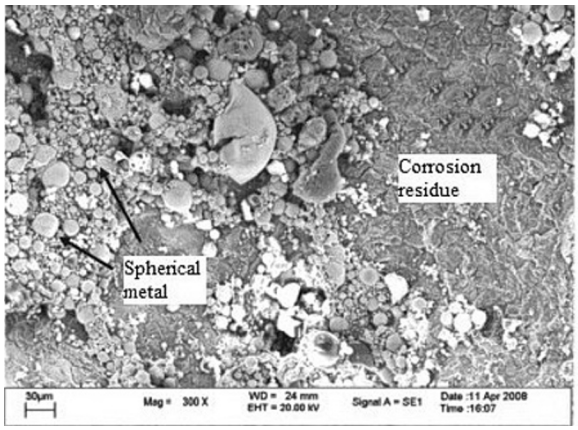

Fig. 1. SEM image of the internal surface of corrosion pit A.

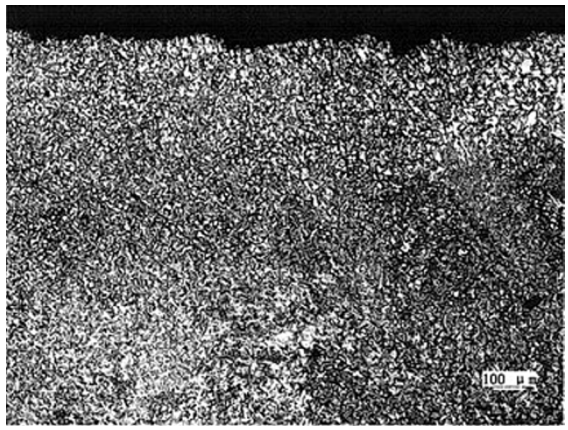

Fig. 2. SEM image of the surface of the nitriding layer.

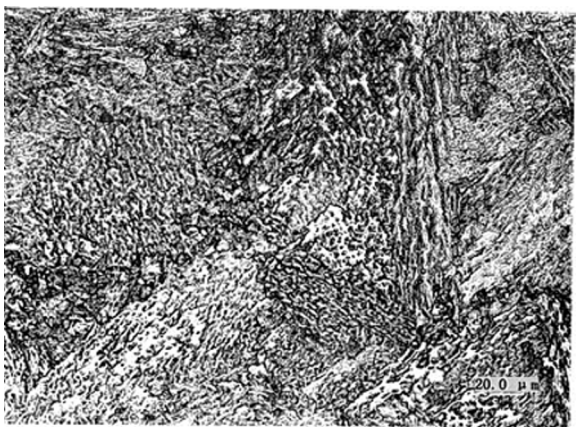

Fig. 3. SEM illustration of the cross-section of the nitrided layer.

2. Micrograph of Corroded Sites.

2.1. Morphology of Internal Surface of Corrosion Pit. As illustrated in Fig. 1, the corrosion pit was covered with cracked residues and spheres. It was analyzed that these spheres were molten molybdenum wires for cutting which were splashed into the corrosion pit and cooled.

2.2. Morphology of the Surface of Nitriding Layer. The surface of the nitriding layer consisted of blocky ferrite (white) and tempered sorbite (Fig. 2). Oxidative corrosion took place along the boundaries of ferrite grains, i.e., intergranular corrosion. The nitrided layers also contained small amounts of particulate nitrogen-carbon compounds, resulting from a low quenching temperature of the sampling point during thermal treatment.

2.3. Morphology of Cross-Section of the Nitrided Layer. In Fig. 3, the cross-section of the nitrided layer over the cylinder liner compromises large granular bainite and granular nitride. In detail, the texture consists of large tempered sorbite with the orientation of original martensite and little bainite. It is demonstrated that this sampling point was subjected to an exceedingly high quenching temperature, i.e., an overheated texture.

3. Analysis of Corrosion Products and Corrosion Mechanism. The matrix metal species and corrosion products in the cross-section were characterized with energy dispersive spectroscopy (EDS), as depicted in Fig. 4. As a result, the corrosion products are metal oxides.

The wear resistance of the internal surface of the cylinder liner was improved by the nitriding treatment. However, due to the formation of chromium nitrides, the content of chromium in the matrix was reduced, and therefore the oxidation resistance and corrosion resistance of the matrix were reduced. Affected by the high-temperature flue gas under the working condition, the cylinder liner was corroded by grain boundary oxidation, resulting in

TABLE 1. EDS Composition Analysis of Corrosion Products

Regional		Chemical composition							
		O	Si	Cr	Mn	Fe	Ni	Mo	W
1	wt.%	–	0.63	2.69	0.69	94.98	1.01	–	–
	at.%	–	1.24	2.87	0.70	94.24	0.96	–	–
2	wt.%	23.51	1.11	12.04	0.69	52.71	–	2.15	7.79
	at.%	53.20	1.43	8.39	0.46	34.18	–	0.81	1.53
3	wt.%	–	0.58	2.31	0.85	95.14	1.12	–	–
	at.%	–	1.14	2.46	0.85	94.48	1.06	–	–

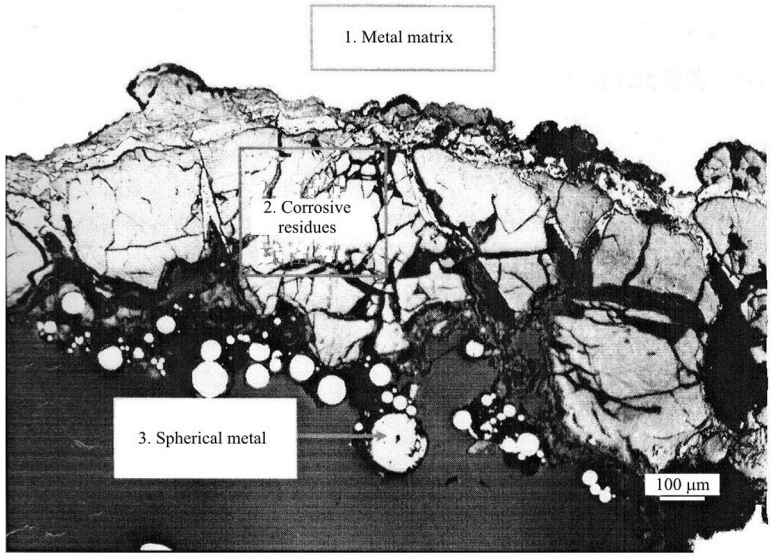

Fig. 4. SEM image of metal species and corrosion products in the surface layer or the substrate.

shallow oxidative corrosion pits. Moreover, the gas vortex was prone to be formed around these corrosion pits, increasing oxidation and corrosion of these pits. Consequently, the oxidation and corrosion would be developed to form inverted-funnel-shaped corrosion pits.

In addition, the nitriding resulted in a bright white nitrogen-containing layer deposited over the surface with great wear resistance, corrosion resistance, and oxidation resistance. To ensure the dimensional accuracy and surface finish of the cylinder liner, we then treated the surface with fine grinding, resulting in the thinning or absence of the nitrogen-containing layer. As a consequence, the wear resistance, corrosion resistance, and oxidation resistance were all decreased.

EDS results on sites A, B, C, and D in Fig. 1 are described in Table 1. Oxides were only generated over the surfaces of sites A, C, and D. viz. only sites A, C, and D were oxidized. The composition of site B was close to that of the substrate.

It is demonstrated in Tables 1 and 2 that the thermal corrosion was ascribed to the chemical reactions between the surface of the cylinder liner and elements (S, O, Ca, etc.) in the flue gas at high temperatures and high pressures.

4. Measurement of the Thickness of Nitriding Layer. The thickness of the nitriding layer was measured with the hardness-gradient method [11]. The cross-section of site E was sampled for the hardness test. The internal surface, with a nitrogen-containing diffusion layer, and external surface, with a bright-white-nitrogen-species-containing nitriding layer, of the sample were both tested. The thickness of the nitriding layer was determined at the location of which the hardness was higher than that of the substrate by 30 HV0.3. Results of the hardness test are depicted in Table 2.

TABLE 2. Hardness Test Results of Substrate Direction

Test site (E)		1	2	3	4	5	6	Matrix hardness	t, mm
Inner surface	D, mm	0.03	0.21	0.34	0.46	0.58	–	–	0.58
	HV0.3	722.4	684.9	517.1	366.6	341.5	–	306.1	–
Outer surface	D, mm	0.06	0.16	0.32	0.60	0.79	0.83	–	0.83
	HV0.3	949.9	908.1	792.1	437.7	386.2	358.1	317.8	–

Note. D is the distance from the surface and t is the nitrided layer thickness.

It is indicated that the nitriding treatment was positive, and the thickness of the nitriding layer over the external surface was much larger than that over the internal surface. This was because the fine grinding had eliminated the bright-white-nitrogen compounds in the internal surface.

Conclusions. The corrosion mechanism of internal surface of the 12Cr2NiWVA alloy was studied under high-temperature and high-pressure circumstances. A stereomicroscope, scanning electron microscope, and microhardness tester were employed to characterize the corrosion and morphology of the internal surface. The influence of nitriding, thermal treatment, and fine grinding on corrosion was clarified. The corrosion products were qualitatively analyzed, and cross-sectional hardness was measured.

Under operational conditions, the high-temperature flue gas will lead to grain boundary oxidation and corrosion, resulting in shallow oxidation corrosion pits. Gas vortex is easily formed around the corrosion pits, which causes oxidation and corrosion of these pits, resulting in developed oxidation and corrosion. Fine grinding thins or eliminates bright-white-nitrogen-species-containing layers, leading to the reduction of wear resistance, corrosion resistance, and oxidation resistance. Besides, the specimen was unevenly heated during the thermal treatment, resulting in different properties after the nitriding and increased deformation of the specimen.

Moreover, an appropriate increase of contents of chromium and aluminum can effectively improve the corrosion resistance, oxidation resistance, and the nitriding effect of materials. By nitriding treatment and post-processing, a layer of the wear-resistant, corrosion-resistant, and oxidation-resistant membrane will be deposited over the cylinder liner, greatly improving the performance of the cylinder liner. This improvement is especially pronounced for the cobalt-chromium-yttrium alloy [2, 12–14].

REFERENCES

1. Z. T. Huang, W. H. Tian, and Y. G. Su, "Failure analysis of 12Cr2NiWVA steel cylinder under hot corrosion," *Heat Treat. Met.*, **35**, No. 3, 101–103 (2010).
2. M. Kaur, H. Singh, and S. Prakash, "High-temperature corrosion studies of HVOF-sprayed Cr_3C_2-NiCr coating on SAE-347H boiler steel," *J. Therm. Spray Tech.*, **18**, No. 4, 619–632 (2009).
3. X. M. Huang, "How to raise the ability of resisting cave corrosion on marine diesel cylinder sleeve," *Internal Combustion Engines*, No. 1, 51–52 (2006).
4. K. Weulersse, G. Moulin, P. Billard, and G. Pierotti, "High temperature corrosion of superheater tubes in waste incinerators and coal fired," *Mater. Sci. Forum*, **461–464**, 973–980 (2004).
5. Z. H. Na, "Diesel engine cylinder liner cavitation and prevention," *HEI LONG JIANG JIAO TONG KE JI*, **26**, No. 8, 15–17 (2004).
6. T. S. Sidhu, S. Prakash, and R. D. Agrawal, "Hot corrosion studies of HVOF sprayed Cr_3C_2–NiCr and Ni–20Cr coatings on nickel-based superalloy at 900℃," *Surf. Coat. Tech.*, **201**, Nos. 3–4, 792–800 (2006).
7. S. W. Li, L. F. Huang, and Q. L. Meng, "Study on quality characteristics of molybdenum wires for WEDM," *Mach. Mold*, No. 4, 63–67 (2013).
8. N. Espallargas, J. Berget, J. M. Guilemany, et al., "Cr_3C_2-NiCr and WC-Ni thermal spray coatings as alternatives to hard chromium for erosion-corrosion resistance," *Surf. Coat. Tech.*, **202**, No. 8, 1405–1417 (2008).

9. C. Liang, “SEM-EDS analysis of fiber surface of sulfonated chemimechanical pulps,” *Paper Sci. Technol.*, No. 31, 110–114 (2012).
10. R. A. Mahesh, R. Jayaganthan, and S. Prakash, “Microstructural characterization and hardness evaluation of HVOF sprayed Ni–5Al coatings on Ni- and Fe-based superalloys,” *J. Mater. Process. Tech.*, **209**, No. 7, 3501–3510 (2009).
11. G. Z. Shen, “Bending behavior based on hardness gradient for hot forming high strength steel,” *Trans. Chin. Soc. Agricult. Mach.*, No. 44, 261–266 (2013).
12. I. Gurrappa, I. V. S. Yashwanth, and A. K. Gogia, “The behaviour of superalloys in marine gas turbine engine conditions,” *J. Surf. Eng. Mater. Adv. Technol.*, **1**, No. 3, 144–149 (2011).
13. I. Gurrappa, I. V. S. Yashwanth, and A. K. Gogia, “The selection of materials for marine gas turbine engines,” in: K. Volkov (Ed.), *Efficiency, Performance and Robustness of Gas Turbines*, InTech (2012), pp. 51–70.
14. Z. Y. Ren, J. Q. Xin, and C. L. Zhan, “Main measurements of improving ferritic stainless steels,” *Shanxi Metallurgy*, No. 2, 31–32 (2005).